ACS OMEGA

http://pubs.acs.org/journal/acsodf

Article

Construction of a Phenylboronic Acid-Functionalized Nano-Prodrug for pH-Responsive Emodin Delivery and Antibacterial Activity

Guodong Zheng,[‖] Jiahui Zheng,[‖] Le Xiao,[‖] Tongyi Shang, Yanjun Cai, Yuwei Li, Yiming Xu, Xiaoming Chen, Yun Liu,* and Bin Yang*

Cite This: *ACS Omega* 2021, 6, 8672−8679

Read Online

ACCESS | Metrics & More | Article Recommendations

ABSTRACT: In this study, a pH-responsive nano-prodrug was fabricated by conjugating emodin to the PEGylated polyethyleneimine (mPEG-PEI) with acid-sensitive boronate ester bonds. ^{1}H NMR spectra results showed that emodin was effectively bonded to mPEG-PEI, and acid-sensitive assay further confirmed the formation of boronate ester bonds. The size and morphology of the nano-prodrug were ascertained through transmission electron microscopy (TEM) and dynamic light scattering (DLS), which showed that the prodrug has a sphere-like shape with hydrodynamic size around 102 nm at pH 7.4. Subsequently, a drug-release behavior assay was carried out to carefully investigate the acid-sensitive drug-delivery property of the prodrug. Moreover, in vitro cell viability assay confirmed the superior cytotoxic effect of the nano-prodrug against HeLa cells compared to free emodin. Furthermore, the antibacterial study showed that the nano-prodrug could inhibit the bacterial (both Gram-positive and Gram-negative) growth more effectively than free emodin. Overall, this study provides a promising paradigm of the multifunctional nano-prodrug for pH-responsive tumor therapy and antibacterial activity.

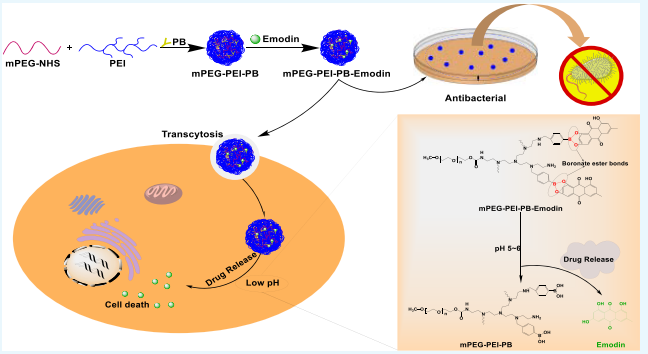

1. INTRODUCTION

Cancer is one of the most important diseases with high morbidity and mortality in the 21st century.[1] In 2020, 1 806 590 new cancer cases and 606 520 cancer-associated deaths were projected to occur in the United States by the National Center for Health Statistics,[2] and the rapidly increasing cancer-associated morbidity and mortality are now ranked second among most common diseases in the United States (just after heart disease).[3] Moreover, cancer is the second most common cause of death among old people after cardiovascular disease.[4] In general, traditional treatment methods such as surgery, chemotherapy, and radiotherapy can serve as relatively effective strategies for clinical cancer therapy, while the existence of a wide range of damage or high toxic side effects to the patients can greatly limit their applications in a variety of cases of clinical therapy.[5−7] As for cancer chemotherapy, poor pharmacokinetic properties and embarrassed toxic side effects restrain its further development. Cancer nanomedicine has been developed to overcome the limitations associated with conventional drugs. Nanomedicine involves the application of nanoscale materials for diagnosis and treatment of cancer with the ability to preferentially accumulate in the tumor sites by enhanced permeability and retention (EPR) effect. To date, several nanomedicines have been used in clinical practice and have shown improved drug solubility, prolonged circulation, enhanced bioavailability, and reduced adverse effects.[8]

Similar to cancer, pathogenic bacteria-related diseases also pose a great threat to the human health. More importantly, the emergence of drug-resistant bacteria made the situation increasingly challenging.[9] It has become an urgent need to develop antibacterial materials against bacterial infection. Based on these situations, several effective antibacterial strategies have been proposed, such as amphiphilic polymers, inorganic complexes, natural products, and other smart therapeutic systems.[10−13] Nanosized antibacterial materials with high surface area and high reactivity have shown better effect in inhibiting the growth and reproduction of bacteria.[14−16] In general, antibacterial nanomaterials with stable structure, good biocompatibility, high drug-loading efficiency, and smart sensitivity should be developed to meet the clinical requirements.

Received: February 2, 2021
Accepted: March 10, 2021
Published: March 18, 2021

https://doi.org/10.1021/acsomega.1c00606
ACS Omega 2021, 6, 8672−8679

Scheme 1. Schematic Design of PPPE Nano-prodrug for pH-Responsive Emodin Delivery and Antibacterial Activity[a]

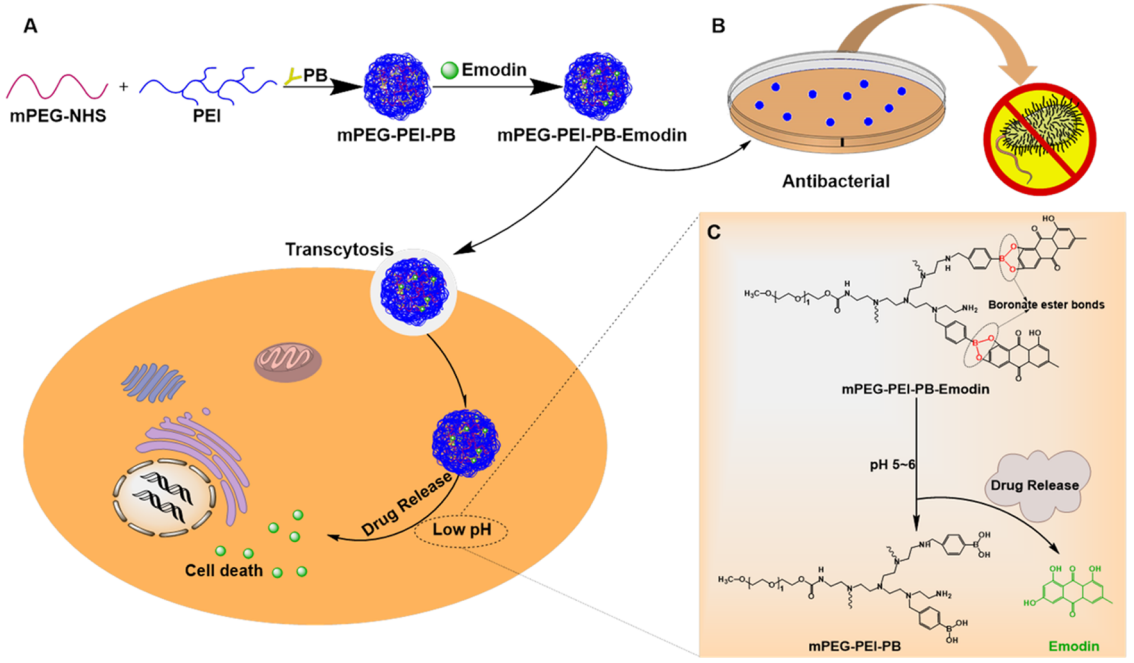

[a](A) pH-sensitive boronate ester bridged emodin nano-prodrug for anticancer drug-delivery system. (B) Antibacterial activity of the nano-prodrug. (C) Illustration of drug-release mechanism of the PPPE under weak-acidic environment.

As a drug combining antitumor and antibacterial properties, Emodin (1,3,8-trihydroxy-6-methylanthraquinone), found to be a main active ingredient in different Chinese herbs (including *Rheum palmatum*, *Polygonum multiflorum*, *Polygonam multiflorum*, etc.),[17,18] is a natural occurring anthraquinone derivative extracted from barks and roots of molds, lichens, and numerous plants. It is a polyvalent molecule with a variety of bioactivities such as inhibition of oxidative stress,[19] anti-inflammatory,[20,21] antibacterial,[22] and most importantly, antitumor effects have been confirmed to act against several types of cancers including colorectal cancer,[23] breast cancer,[24] and glioma.[25] Furthermore, recent studies have demonstrated that emodin has the ability to suppress cell proliferation and accelerate apoptosis in a variety of tumor cells,[26] induce autophagy,[27] or inhibit tumor metastasis.[28] These pharmacological properties of emodin indicate that it might be a valuable medicine for prophylaxis and treating multiple diseases in the human body. However, reports have emerged that emodin has some toxic side effects on the human body, such as hepatotoxicity,[29] genotoxicity,[30] embryonic toxicity,[31] etc. How to improve these characteristics of emodin has become an urgent problem to be solved.

Prodrugs is a concept first introduced by Adrien Albert in 1958 to improve the undesirable properties of drugs since the late 19th century, which are defined as bio-reversible, inactive derivatives of active drug molecules that release the active parent drug after an enzymatic or chemical transformation in vivo, subsequently eliciting their desired pharmacological effects in the body. The parent drugs commonly show undesirable drug properties, including low solubility in water or lipid membranes, short half-life, poor bioavailability, high toxicity, and so on, but on the contrary, prodrugs reasonably designed can greatly increase the bioavailability and therapeutic effectiveness of parent drug.[32] To date, prodrug-based delivery systems have gained considerable attention owing to their dominant properties helping to overcome the barriers of traditional therapeutic delivery systems including anticancer[33−35] and antibacteria.[36,37] Thus, the prodrug strategy offers a feasible way to improve the absorption, distribution, metabolism, and excretion properties of investigational drugs. In this study, phenylboronic acid (PB) polymers were utilized, which can bind compounds containing diol moieties involving carbohydrates, polyphenols, and glycans in aqueous systems to form boronate ester bonds. They have been widely studied in drug delivery owing to their pH-responsive reversible properties and acidity-accelerated drug-release behavior.[38−40] Currently, a large number of studies are mainly focusing on the anticancer properties of these polymers.[41−44] For example, Zhang et al. developed a pH-responsive gene carrier for photothermally promoted gene delivery.[45] They modified polydopamine nanoparticles (PDANPs) with low-molecular-weight polyethylenimine ($PEI_{1.8k}$) and poly(ethylene glycol)-phenylboronic acid (PEG-PB) to prepare a pH-responsive gene carrier PDANPs-PEI-rPEG. The obtained PDANPs-PEI-rPEG show good performance in gene delivery and realize photothermally promoted gene therapy. Moreover, phenylboronic acid moieties were also introduced in gene/drug co-delivery nanoformulations to improve the anticancer efficiency of the formed vehicle utilizing its enhanced interaction with the cellular membrane by phenylboronic acid moieties.[46,47] Considering the pH-responsive phenylboronic acid−diol coupling strategy and prodrug concept, herein, we constructed a PB-functionalized nano-prodrug for pH-responsive emodin delivery and antibacterial activity (Scheme 1). PB-modified PEGylated polyethyleneimine (mPEG-PEI-PB) was first synthesized. Subsequently, emodin was conjugated to mPEG-PEI-PB by virtue of formation of boronate ester bonds to obtain PB-functionalized nano-prodrug mPEG-PEI-PB-emodin (PPPE) (as shown in Figure 1). The size and morphology of

https://doi.org/10.1021/acsomega.1c00606
ACS Omega 2021, 6, 8672−8679

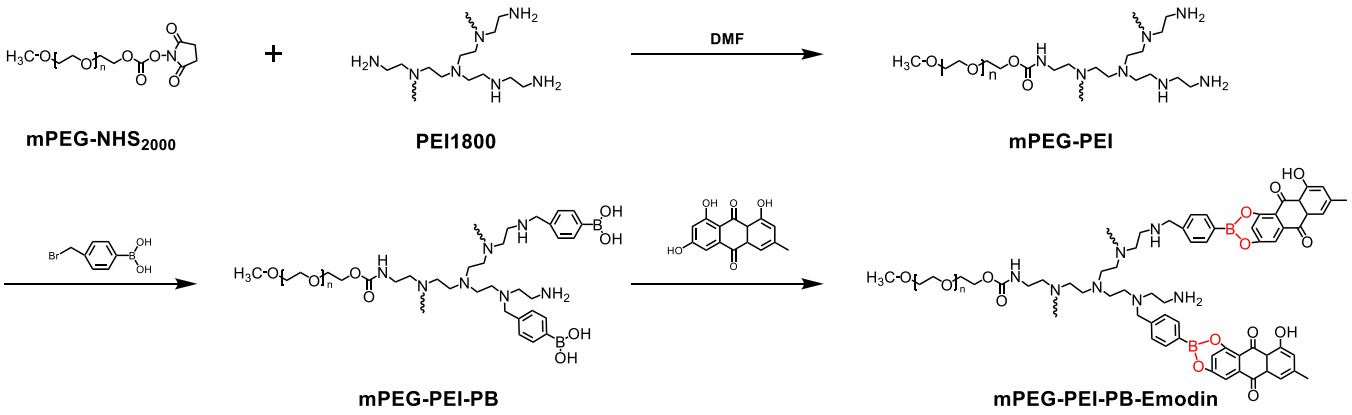

Figure 1. Synthesis routes of mPEG-PEI-PB-emodin nano-prodrug.

the synthesized prodrug were investigated by DLS and TEM, respectively. Moreover, the stimulus-responsive drug-release behaviors, in vitro cellular viability, and the antibacterial activities (both Gram-positive and Gram-negative) were also investigated.

2. RESULTS AND DISCUSSION

2.1. Synthesis and Characterization of the PPPE Prodrug. The chemical structures of all of the synthetic polymers above were characterized by ^{1}H NMR spectrum (Bruker). As shown in Figure 2A, characteristic peaks of

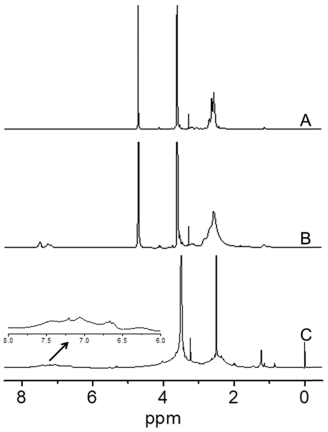

Figure 2. ^{1}H NMR spectra of mPEG-PEI (A) and mPEG-PEI-PB (B) in D_2O, and mPEG-PEI-PB-emodin in DMSO-d_6 (C).

mPEG and PEI were clearly visible at 3.56 and 2.20−3.00 ppm, respectively (assigned to the $-O-CH_2-CH_2-$ in mPEG and $-CH_2-CH_2-NH-$ in PEI), which confirmed the successful conjugation of mPEG and PEI. From the integration ratio of the peaks at 3.56 and 2.20−3.00 ppm, it was estimated that approximately one mPEG was conjugated to the branched chain of each PEI, indicating the successful formation of mPEG-PEI. Similarly, for mPEG-PEI-PB (Figure 2B), the peaks at 7.00−8.00 ppm were belonging to the benzene structure of the PB group, and the grafting degree of PB is about 7 according to the integration area. After the formation of prodrug with emodin, new peaks appeared at 6.00−7.20 ppm, suggesting the successful formation of boronate ester bonds between mPEG-PEI-PB and emodin, and the amount of drug conjugated to the polymer is calculated to be 6 (Figure 2C).

The hydrodynamic diameter and morphology of the conjugated nano-prodrug PPPE were studied by DLS and TEM, respectively. The average hydrodynamic diameter of PPPE determined by DLS was ∼102.8 ± 12 nm, and the polydispersity index (PDI) was 0.264 ± 0.025 (Figure 3A),

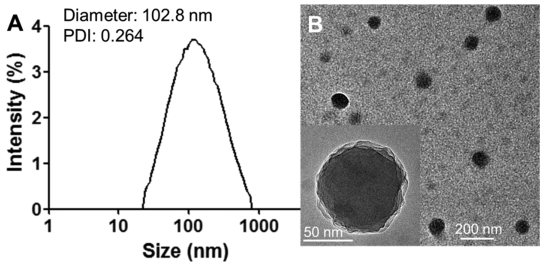

Figure 3. Particle size and morphology of nano-prodrug. (A) Particle size and size distribution measured by DLS. (B) TEM images of PPPE prodrug at different scale bars.

which indicates that the synthesized PPPE has good homogeneity. In addition, the sphere-like shape of the conjugated copolymer PPPE was observed by TEM and its average diameter was consistent with the result of DLS data (Figure 3B). On the contrary, the nanostructure of prodrug was destabilized and could not be detected at pH = 5.0, suggesting the acid-responsiveness of boronate ester bond of prodrug.

2.2. In Vitro Drug-Release Studies. The drug-loading content (DLC) of the PPPE prodrug was ∼23% according to the ^{1}H NMR spectrum (Figure 2C). UV−vis spectrophotometer analysis further confirmed the DLC of PPPE calculated by ^{1}H NMR spectrum. To improve the disadvantages of emodin drug, acid-sensitive boronate ester bond was utilized to endow free emodin with favorable characteristics such as good biocompatibility, high water solubility, lower cytotoxicity, and more importantly, its acid-functionalized modification renders pH-responsive drug release under weak-acid environment, especially in intratumoral weak-acid environment, which is a key point for antitumor behavior of the prodrug. Given the pH-responsive boronate ester bond inside the formed prodrug, its decomposition under the weak-acid environment of tumor tissues could allow the disassembly of the prodrug. Therefore, the targeting selectivity of this drug was improved. To evaluate the pH-sensitive drug-release performance of PPPE, emodin release profiles of the prodrug in vitro were investigated at 37 °C in PBS under different pH

https://doi.org/10.1021/acsomega.1c00606
ACS Omega 2021, 6, 8672−8679

conditions (pH 5.0 and 7.4). After the isolation of release emodin from PPPE via the purification method, the cumulative drug-release percentage of emodin, namely, the total release of emodin over time, was detected by UV−vis spectrophotometry.

As shown in Figure 4, emodin released from the PPPE prodrug exposing under a neutral condition of pH 7.4 after 120 h incubation at 37 °C showed a slow-release behavior with less than ∼40% released emodin detected and then followed by one plateau period. However, PPPE exhibited a rapid release behavior when in aqueous solution at pH 5.0. The cumulative released drug of PPPE was quickly reached up to over ∼80% after 120 h incubation at 37 °C, indicating dominant pH-responsive behavior of PPPE in weak-acid environment. Consequently, the pH-responsive drug-delivery system could facilitate the accumulation of drugs in tumor tissues and hence greatly improve cancer therapeutic efficiency.[48] Similarly, bacteria usually grow faster in acidic environment and the pH-responsive drug release would be more effective to inhibit the bacteria growth compared to a normal neutral environment.

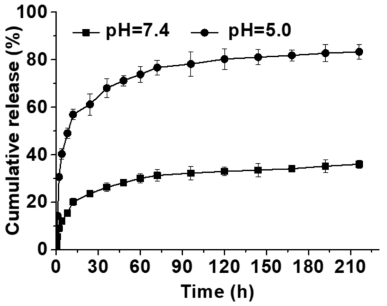

Figure 4. pH-responsive drug-release profiles of emodin from PPPE under different pH values (7.4 and 5.0). Data are presented as mean ± standard deviation (n = 3).

2.3. In Vitro Cytotoxicity Study. To evaluate the in vitro cytotoxicity profiles of PPPE prodrug as well as the in vitro biocompatibility and pharmacological activity of mPEG-PEI and mPEG-PEI-PB to HeLa cells, MTT assay was executed using a series of gradient concentrations of these nanoparticles. As shown in Figure 5A, the biosafety of the synthesized polymers was determined after 48 h of incubation with a series of concentrations of mPEG-PEI and mPEG-PEI-PB (0, 5.2, 7.8, 11.7, 17.6, 26.3, 39.5, 59.3, 88.9, 133.3, and 200 μg mL^{-1}), which indicated no potential cytotoxicity of both mPEG-PEI and mPEG-PEI-PB against HeLa cells. The viability of HeLa cells still remained above ∼80% at a maximum dose of 200 μg mL^{-1}, and besides, the cytotoxicity of mPEG-PEI-PB toward HeLa cells was slightly higher than that of mPEG-PEI, which is probably associated with the boronic acid−carbohydrate interaction.[49] In contrast, the viability of HeLa cells treated with PPPE prodrug nanoparticles and free emodin remarkably decreased as concentration increased, causing pronounced cell death (Figure 5B). Notably, the half-maximal inhibitory concentration (IC50) of PPPE is ca. 7.56 μg mL^{-1} lower than that of free emodin (8.93 μg mL^{-1}), indicating the superior cytotoxic effect of PPPE prodrug against HeLa cells compared to free emodin. Such an enhanced inhibiting effect of PPPE prodrug toward HeLa cells could mainly contribute to the following two causes. First, the PPPE prodrug was more likely internalized by cancer cells compared to free emodin, leading to a higher accumulation concentration of emodin inside cancer cells. Second, the acid-responsive rapid emodin release of PPPE prodrug within weak-acidic organelles could drastically improve the anticancer effect of emodin, which may simultaneously contribute to the higher cytotoxicity of mPEG-PEI-PB to HeLa cells than mPEG-PEI as mentioned above. In contrast, PPPE prodrug was treated with NH_4Cl to block the progression of endosome−lysosome acidification,[40] which actually reduced the release of drug and less cytotoxicity was shown compared to PPPE without NH_4Cl treatment. Therefore, the synthesized PPPE will be a promising prodrug for pH-responsive delivery to cancer cells for high-effect cancer therapy.

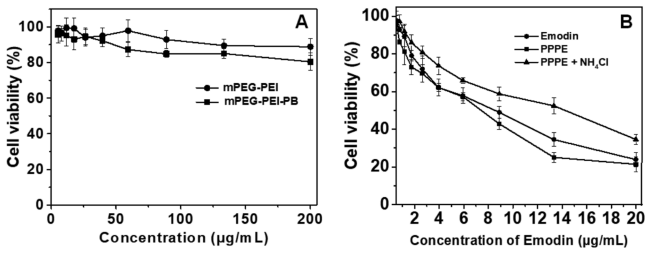

Figure 5. Cell viability of HeLa cells measured using the standard MTT assay treated with mPEG-PEI and mPEG-PEI-PB (A) and free emodin and PPPE (in the absence and presence of 50 mM NH_4Cl) at the same concentration of emodin (B). Data are presented as mean ± standard deviation (n = 4).

2.4. In Vitro Antibacterial Activity. Based on the standard broth microdilution method, in vitro bacterial inhibition assay was performed with *E. coli* and *S. aureus*. The colony-forming unit (CFU) values of each group were observed to decrease with increasing concentrations of both emodin and PPPE. As shown in Figure 6, compared with the control group, the bacterial colony formation was almost completely inhibited when the bacterial suspension was co-cultured with PPPE overnight, especially for *E. coli* at pH 5.0. On the whole, the bacterial inhibition ability of the PPPE

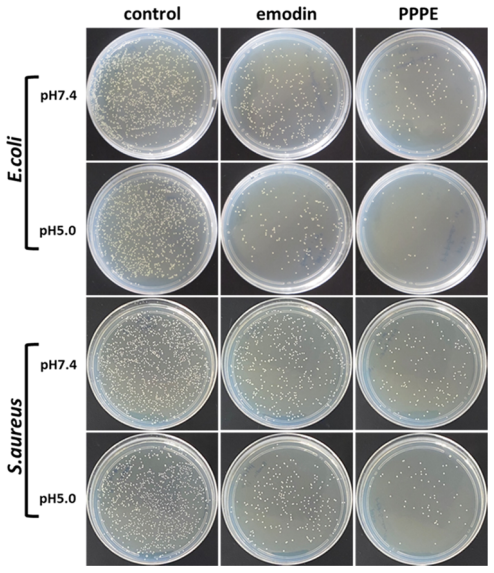

Figure 6. Bacterial colony formation of *E. coli* and *S. aureus* treated with emodin and PPPE prodrug at pH 7.4 and 5.0. The concentration of emodin was kept the same in all samples.

https://doi.org/10.1021/acsomega.1c00606
ACS Omega 2021, 6, 8672−8679

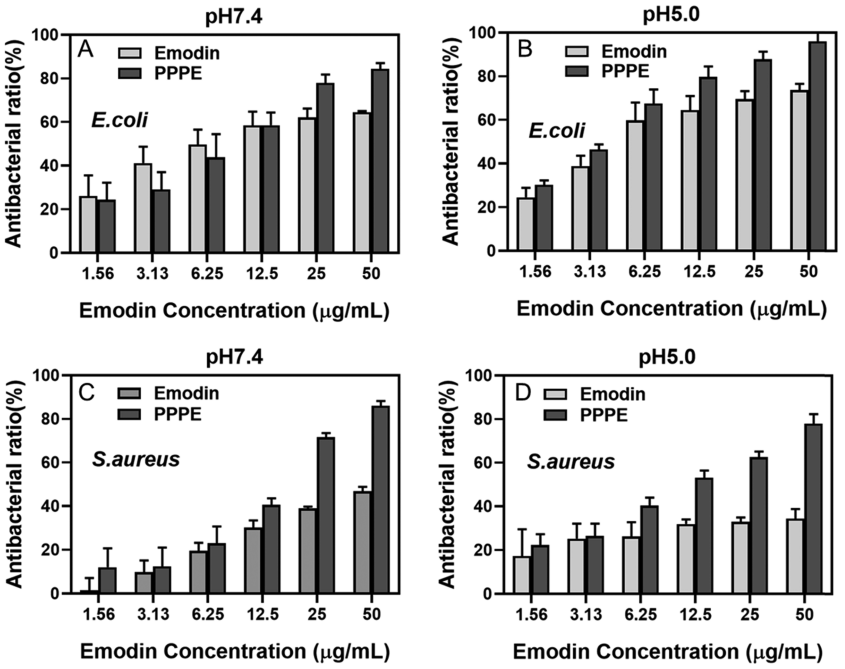

Figure 7. Quantitative results of antibacterial activity toward *E. coli* (A, B) and *S. aureus* (C, D) with emodin and PPPE prodrug at pH 7.4 (A, C) and pH 5.0 (B, D). The concentration of emodin was kept the same in all samples.

group was better than the group of free emodin, and acidic environment further inhibited the bacterial growth, which is owing to the pH-responsive property of the prodrug and thus accelerated emodin release. The bacterial inhibition ratios of emodin were about 73.7 and 34.4% in pH 5.0 against *E. coli* and *S. aureus*, respectively, while the corresponding inhibition ratios of PPPE were increased to 96.0 and 78.0% (Figure 7). The difference between *E. coli* and *S. aureus* could be attributed to the bacteria-dependent inhibition ability. All of the above results suggest that conjugation of small molecule emodin to polymeric structure and the formation of nano-prodrug could greatly improve its antibacterial effect. Cationic molecules can be adsorbed onto the anionic surface of bacteria membrane through charge interactions.[50] The high antibacterial ability of this nano-prodrug might also be related to the positively charged PEI unit that could efficiently bind with negatively charged bacteria surface by electrostatic interaction.[51,52]

3. CONCLUSIONS

In conclusion, an emodin-associated pH-responsive nano-prodrug was fabricated and the in vitro anticancer activity as well as antibacterial effect was investigated in this study. First, methoxy poly(ethylene glycol) (mPEG) was conjugated with hyperbranched polyethyleneimine (PEI) to improve the biocompatibility of the polymer, and then PEGylated PEI was conjugated with emodin by acid-sensitive boronate ester bond. This nano-prodrug can self-assemble into spherical nanoparticles in an aqueous system and release drug quickly in the weak-acidic tumor environment. At the same time, the rational designed polymeric nano-prodrug provides a promising paradigm of multifunctional nanomedicine for pH-responsive tumor therapy and antibacterial activity.

4. EXPERIMENTAL SECTION

4.1. Materials. Methoxy poly(ethylene glycol)-*N*-hydroxysuccinimide (mPEG-NHS, 2000 Da), poly(ethylenimine) (PEI, 1800 Da), 4-(bromomethyl)phenylboronic acid (PB), and emodin were purchased from Aladdin Industrial, Inc. Cell culture medium and trypsin EDTA Solution A were purchased from Biological Industry (Belgium). Buffer solution (acetic acid/sodium acetate), PBS, and various solvents were purchased from Sinopharm Chemical Reagent Co., Ltd. Deionized water was used in all of the experiments, and it was obtained using a Millipore water purification system. All reagents and buffer solution components were of analytical grade.

4.2. Preparation of mPEG-PEI. Methoxy poly(ethylene glycol)-*b*-polyethyleneimine was abbreviated as mPEG-PEI in this paper. mPEG-PEI was prepared according to the method previously described in the literature.[53−55] In this work, the relative optimized feed molar ratio of the mPEG and PEI was about 1:1. Briefly, PEI (336 mg) and mPEG-NHS (336 mg) were separately dissolved in 10 mL of *N*,*N*-dimethylformamide (DMF), and then mPEG-NHS solution was added dropwise to the PEI solution and stirred at 50 °C. After 24 h, the reaction solution was dialyzed (MWCO 3.5 kDa) against distilled water for 2 days and finally lyophilized and kept at 2−8 °C until used in the subsequent reaction. The final product was a white solid that was characterized by ^{1}H NMR. The ^{1}H NMR spectrum of the mPEG-PEI was obtained on a Bruker AVANCE NEO 300 MHz spectrometer using D_2O as the solvent.

4.3. Synthesis of mPEG-PEI-PB. The polymer was synthesized according to the method reported before.[47,56] Briefly, mPEG-PEI (282 mg) was dissolved in 20 mL of methanol, and then excess 4-(bromomethyl)phenylboronic acid (PB) (127.5 mg) was added into the mixture and stirred at ∼76 °C. The feed molar ratio of mPEG-PEI and PB was 1:8. After 24 h, methanol was removed utilizing reduced-pressure distillation, and a light-yellow viscous sample was obtained. Then, the sample was transferred to a dialysis bag (MWCO, 3.5 kDa) and dialyzed against 2000 mL of deionized water for 24 h. mPEG-PEI-PB was finally obtained after lyophilization.

https://doi.org/10.1021/acsomega.1c00606
ACS Omega 2021, 6, 8672−8679

4.4. Conjugation of Prodrug. The nano-prodrug PPPE was synthesized using a previously reported method.[43,57,58] Emodin (104 mg) and mPEG-PEI-PB (236 mg) were added to the solvent containing 30 mL of DMF and 4 mL of methanol at 40 °C. After reaction for 24 h, methanol was removed utilizing reduced-pressure distillation, and then the sample was transferred to a dialysis bag (MWCO, 3.5 kDa) against distilled water for 2 days to remove free emodin. The PPPE was obtained after lyophilization.

4.5. Characterization of PPPE Prodrug. The hydrodynamic diameter and the polydispersity of PPPE self-assembled nanoparticles were measured under the conditions of pH 7.4 and 5.0 using a DLS system (Zetasizer Nano-ZS; Malvern Instruments). The morphology and size of the nanoparticles were measured by TEM performed on an FEI Tecnai G2 20 TWIN electron microscope operating at an acceleration voltage of 200 kV.

4.6. Drug-Release Behavior. The absorption peaks of emodin were measured by a UV−vis spectrophotometer (UV-5100B, METASH), and the UV absorbances of different concentrations were recorded to plot the free emodin standard curve at the absorption peaks. Then, PPPE was dissolved in an appropriate amount of dimethyl sulfoxide (DMSO). The solution was collected for UV−vis spectrophotometry analysis to measure the absorbance at 430 nm. The drug-loading content of emodin was calculated according to the following equation

$$\text{DLC}\ (\%) = (\text{mass of loaded drug}/\text{mass of nano} - \text{prodrug}) \times 100 \quad (1)$$

The in vitro release study of emodin from the prodrug was investigated using the dialysis method under a simulated physiological environment. First, 15 mg of PPPE was dissolved at 1.5 mL of PBS under different pH conditions (pH 5.0 and 7.4, respectively). The PPPE solution was transferred into a dialysis bag (MWCO 3.5 kDa) and immersed in 30 mL of PBS, followed by incubation at 37 °C in a shaker. Subsequently, 4 mL of the sample was withdrawn from the centrifuge tube at predetermined different time points. For each 4 mL of aliquot sample, an equal volume of fresh PBS solution was replaced. Finally, the UV−vis absorbance of the collected samples was tested at 430 nm. The mass of the released emodin was determined by the free emodin standard curve. All experiments were performed in triplicate.

4.7. Cell Viability Assay. MTT (3-(4,5-dimethylthiazol-2-yl)-2,5-diphenyltetrazolium bromide) assay was carried out to evaluate the antitumor performance of PPPE prodrug. For a comparative study, mPEG-PEI and mPEG-PEI-PB without emodin loading were also studied. Cellular viability test was examined using the MTT assay with HeLa cells. HeLa cells were grown in Dulbecco's modified Eagle's medium (DMEM) (supplemented with 10% fetal bovine serum) culture medium, 10% (w/v) penicillin−streptomycin, and 1% (w/v) Glutamineat at 37% under a humidified atmosphere with 5% CO_2 for 24 h. To investigate the characteristics of these polymers preferably, the MTT assay was divided into two groups. For the first group, the culture media was replaced with 100 μL of DMEM culture media containing mPEG-PEI and mPEG-PEI-PB with gradient concentrations. In the second group, the culture media was replaced with 100 μL of DMEM culture media containing free emodin and PPPE prodrug with same concentrations of emodin (in the absence and presence of 50 mM NH_4Cl). Four multiple wells were set for each sample. After incubation for 48 h, the cells were washed with PBS (pH 7.4), and each well was treated with 20 μL of MTT (5 mg mL^{-1}) solution at 37 °C for 4 h. Then, the medium containing MTT was replaced with 150 μL of DMSO to dissolve the formed formazan crystals. Finally, the absorbance of the sample was measured using a microplate reader (TOM-3MK, TOMOS) at 570 nm. The cell viability (%) was analyzed and calculated using the following equation

$$\text{cell viability}\ (\%) = (\text{OD}_{\text{sample}} - \text{OD}_{\text{control}})/(\text{OD}_{\text{control}}) \times 100 \quad (2)$$

4.8. In Vitro Antibacterial Experiment. Both *E. coli* and *S. aureus* were applied to evaluate the antibacterial activity of emodin and PPPE through bacterial inhibition assays and the spread plate method in standard Luria Bertani (LB) medium at 37 °C. For bacterial inhibition assays, the bacterial inhibition ratios were determined by measuring the survival rate of bacteria in LB medium. That is to say, several colonies of *E. coli* or *S. aureus* on an LB agar plate were transferred to 5 mL of LB liquid culture medium, and then the bacteria suspension was diluted with LB liquid medium to approximately 1.5×10^6 CFU mL^{-1}. In addition, a series of 2-fold dilution dispersion of emodin (50, 25, 12.5, 6.25, 3.13, 1.56 μg mL^{-1}) and PPPE (at an equivalent dosage gradient to emodin) were prepared and added to an equal volume of bacteria suspensions (0.1 mL) in each well of a 96-well plate and incubated at 37 °C overnight. Finally, the absorbance of live bacteria in each well of a 96-well plate was determined by a microplate reader in 600 nm wavelength. Growth medium containing only microbial cells was used as the negative control. Each bacterial inhibition test was carried out in three replicate and repeated three times, and inhibition ratios were calculated according to the following equation

$$\text{bacterial inhibition ratio}\ (\%) = (\text{OD}_{\text{control}} - \text{OD}_{\text{sample}})/(\text{OD}_{\text{control}}) \times 100 \quad (3)$$

For spread plate assays, bacterial suspensions (1.5×10^6 CFU mL^{-1}) were mixed with different samples. Then, they were cultured in a shaker at 37 °C overnight. Then, the bacterial suspension was further diluted 10^4 times by PBS. Finally, 10 μL of diluted bacterial suspension was added onto a solid medium by the spread plate method and cultured at 37 °C overnight.

AUTHOR INFORMATION

Corresponding Authors

Yun Liu − *Guangdong Key Laboratory for Research and Development of Natural Drugs, Guangdong Medical University, Zhanjiang 524023, P. R. China*; Email: liuyun_2017@hotmail.com

Bin Yang − *The Sixth Affiliated Hospital of Guangzhou Medical University, Department of Biomedical Engineering, School of Basic Medical Sciences, Guangzhou Medical University, Guangzhou 511436, P. R. China*; orcid.org/0000-0001-9416-3094; Email: bin.yang@gzhmu.edu.cn

Authors

Guodong Zheng − *The Sixth Affiliated Hospital of Guangzhou Medical University, Department of Biomedical*

https://doi.org/10.1021/acsomega.1c00606
ACS Omega 2021, 6, 8672−8679

Engineering, School of Basic Medical Sciences, Guangzhou Medical University, Guangzhou 511436, P. R. China

Jiahui Zheng − *School of Pharmaceutical Sciences, Guangzhou Medical University, Guangzhou 511436, P. R. China*

Le Xiao − *Guangdong Key Laboratory for Research and Development of Natural Drugs, Guangdong Medical University, Zhanjiang 524023, P. R. China*

Tongyi Shang − *The Sixth Affiliated Hospital of Guangzhou Medical University, Department of Biomedical Engineering, School of Basic Medical Sciences, Guangzhou Medical University, Guangzhou 511436, P. R. China*

Yanjun Cai − *The Sixth Affiliated Hospital of Guangzhou Medical University, Department of Biomedical Engineering, School of Basic Medical Sciences, Guangzhou Medical University, Guangzhou 511436, P. R. China*

Yuwei Li − *The Sixth Affiliated Hospital of Guangzhou Medical University, Department of Biomedical Engineering, School of Basic Medical Sciences, Guangzhou Medical University, Guangzhou 511436, P. R. China*

Yiming Xu − *The Sixth Affiliated Hospital of Guangzhou Medical University, Department of Biomedical Engineering, School of Basic Medical Sciences, Guangzhou Medical University, Guangzhou 511436, P. R. China*

Xiaoming Chen − *The Sixth Affiliated Hospital of Guangzhou Medical University, Department of Biomedical Engineering, School of Basic Medical Sciences, Guangzhou Medical University, Guangzhou 511436, P. R. China*

Complete contact information is available at: https://pubs.acs.org/10.1021/acsomega.1c00606

Author Contributions

[‖]G.Z., J.Z., and L.X. contributed equally to this work. The manuscript was written through contributions of all authors.

Notes

The authors declare no competing financial interest.

■ ACKNOWLEDGMENTS

The authors thank the financial support from the Natural Science Foundation of China (51903062), Guangdong Basic and Applied Basic Research Foundation (2020A1515011320), Natural Science Foundation of Guangdong Province of China (2018A030313588), the Open Laboratory Project of Guangzhou Medical University (B185004159), and the Science and Technology Planning Project of Guangdong Province of China (2016B030309002).

■ REFERENCES

(1) Pang, L. Y.; Argyle, D. J. Veterinary oncology: Biology, big data and precision medicine. *Vet. J.* **2016**, *213*, 38−45.

(2) Siegel, R. L.; Miller, K. D.; Jemal, A. Cancer statistics, 2020. *Ca-Cancer J. Clin.* **2020**, *70*, 7−30.

(3) Heron, M.; Anderson, R. N. Changes in the Leading Cause of Death: Recent Patterns in Heart Disease and Cancer Mortality. *NCHS Data Brief* **2016**, *254*, 1−8.

(4) Coll, P. P.; Korc-Grodzicki, B.; Ristau, B. T.; Shahrokni, A.; Koshy, A.; Filippova, O. T.; Ali, I. Cancer Prevention and Screening for Older Adults: Part 2. Interventions to Prevent and Screen for Breast, Prostate, Cervical, Ovarian, and Endometrial Cancer. *J. Am. Geriatr. Soc.* **2020**, *68*, 2684−2691.

(5) Correal, M. L.; Camplesi, A. C.; Anai, L. A.; Bertolo, P. H. L.; Vasconcelos, R. O.; Santana, A. E. Toxicity of a methotrexate metronomic schedule in Wistar rats. *Res. Vet. Sci.* **2020**, *132*, 379−385.

(6) Melnikova, M.; Wauer, U. S.; Mendus, D.; Hilger, R. A.; Oliver, T. G.; Mercer, K.; Gohlke, B. O.; Erdmann, K.; Niederacher, D.; Neubauer, H.; Buderath, P.; Wimberger, P.; Kuhlmann, J. D.; Thomale, J. Diphenhydramine increases the therapeutic window for platinum drugs by simultaneously sensitizing tumor cells and protecting normal cells. *Mol. Oncol.* **2020**, *14*, 686−703.

(7) Metaxa, A. F.; Efthimiadou, E. K.; Kordas, G. Cellulose-based drug carriers for cancer therapy: Cytotoxic evaluation in cancer and healthy cells. *Mater. Lett.* **2014**, *132*, 432−435.

(8) Shang, T. Y.; Yu, X. Y.; Han, S. S.; Yang, B. Nanomedicine-based tumor photothermal therapy synergized immunotherapy. *Biomater. Sci.* **2020**, *8*, 5241−5259.

(9) Brown, E. D.; Wright, G. D. Antibacterial drug discovery in the resistance era. *Nature* **2016**, *529*, 336−343.

(10) Guo, X. J.; Cao, B.; Wang, C. Y.; Lu, S. Y.; Hu, X. L. In vivo photothermal inhibition of methicillin-resistant *Staphylococcus aureus* infection by in situ templated formulation of pathogen-targeting phototheranostics. *Nanoscale* **2020**, *12*, 7651−7659.

(11) Xia, J. M.; Wang, W. J.; Hai, X.; Shuang, E.; Shu, Y.; Wang, J. H. Improvement of antibacterial activity of copper nanoclusters for selective inhibition on the growth of gram-positive bacteria. *Chin. Chem. Lett.* **2019**, *30*, 421−424.

(12) Wang, C. Y.; Zhao, W.; Cao, B.; Wang, Z. X.; Zhou, Q.; Lu, S. Y.; Lu, L. G.; Zhan, M. X.; Hu, X. L. Biofilm-Responsive Polymeric Nanoparticles with Self-Adaptive Deep Penetration for In Vivo Photothermal Treatment of Implant Infection. *Chem. Mater.* **2020**, *32*, 7725−7738.

(13) Cao, B.; Lyu, X. M.; Wang, C. Y.; Lu, S. Y.; Xing, D.; Hu, X. L. Rational collaborative ablation of bacterial biofilms ignited by physical cavitation and concurrent deep antibiotic release. *Biomaterials* **2020**, *262*, No. 120341.

(14) Wu, C. T.; Zhou, Y. H.; Xu, M. C.; Han, P. P.; Chen, L.; Chang, J.; Xiao, Y. Copper-containing mesoporous bioactive glass scaffolds with multifunctional properties of angiogenesis capacity, osteostimulation and antibacterial activity. *Biomaterials* **2013**, *34*, 422−433.

(15) Bari, A.; Bloise, N.; Fiorilli, S.; Novajra, G.; Vallet-Regi, M.; Bruni, G.; Torres-Pardo, A.; Gonzalez-Calbet, J. M.; Visai, L.; Vitale-Brovarone, C. Copper-containing mesoporous bioactive glass nanoparticles as multifunctional agent for bone regeneration. *Acta Biomater.* **2017**, *55*, 493−504.

(16) Müller, D. W.; Losslein, S.; Terriac, E.; Brix, K.; Siems, K.; Moeller, R.; Kautenburger, R.; Mucklich, F. Increasing Antibacterial Efficiency of Cu Surfaces by targeted Surface Functionalization via Ultrashort Pulsed Direct Laser Interference Patterning. *Adv. Mater. Interfaces* **2020**, No. 2001656.

(17) Dong, X. X.; Fu, J.; Yin, X. B.; Cao, S. L.; Li, X. C.; Lin, L. F.; Huyiligeqi; Ni, J. Emodin: A Review of its Pharmacology, Toxicity and Pharmacokinetics. *Phytother. Res.* **2016**, *30*, 1207−1218.

(18) Monisha, B. A.; Kumar, N.; Tiku, A. B. Emodin and Its Role in Chronic Diseases. *Adv. Exp. Med. Biol.* **2016**, *928*, 47−73.

(19) Lee, E. H.; Baek, S. Y.; Park, J. Y.; Kim, Y. W. Emodin in Rheum undulatum inhibits oxidative stress in the liver via AMPK with Hippo/Yap signalling pathway. *Pharm. Biol.* **2020**, *58*, 333−341.

(20) Li, X.; Shan, C.; Wu, Z.; Yu, H.; Yang, A.; Tan, B. Correction to: Emodin alleviated pulmonary inflammation in rats with LPS-induced acute lung injury through inhibiting the mTOR/HIF-1α/VEGF signaling pathway. *Inflammation Res.* **2020**, *69*, 711.

(21) Li, X. Q.; Shan, C.; Wu, Z. H.; Yu, H. J.; Yang, A. D.; Tan, B. Emodin alleviated pulmonary inflammation in rats with LPS-induced acute lung injury through inhibiting the mTOR/HIF-1 alpha/VEGF signaling pathway. *Inflammation Res.* **2020**, *69*, 365−373.

(22) Ji, C. J.; Xin, G.; Duan, F. X.; Huang, W.; Tan, T. C. Study on the antibacterial activities of emodin derivatives against clinical drug-resistant bacterial strains and their interaction with proteins. *Ann. Transl. Med.* **2020**, *8*, 92.

(23) Dai, G. L.; Ding, K.; Cao, Q. Y.; Xu, T.; He, F.; Liu, S. J.; Ju, W. Z. Emodin suppresses growth and invasion of colorectal cancer cells by inhibiting VEGFR2. *Eur. J. Pharmacol.* **2019**, *859*, No. 172525.

(24) Huang, P. H.; Huang, C. Y.; Chen, M. C.; Lee, Y. T.; Yue, C. H.; Wang, H. Y.; Lin, H. Emodin and Aloe-Emodin Suppress Breast Cancer Cell Proliferation through ER alpha Inhibition. *Evidence-Based Complementary Altern. Med.* **2013**, *2013*, No. 376123.
(25) Zhou, J. B.; Li, G. H.; Han, G. K.; Feng, S.; Liu, Y. H.; Chen, J.; Liu, C.; Zhao, L.; Jin, F. Emodin induced necroptosis in the glioma cell line U251 via the TNF-alpha/RIP1/RIP3 pathway. *Invest. New Drugs* **2020**, *38*, 50−59.
(26) Wu, Y. Y.; Zhang, J. H.; Gao, J. H.; Li, Y. S. Aloe-emodin (AE) nanoparticles suppresses proliferation and induces apoptosis in human lung squamous carcinoma via ROS generation in vitro and in vivo. *Biochem. Biophys. Res. Commun.* **2017**, *490*, 601−607.
(27) Liu, H.; Gu, L. B.; Tu, Y.; Hu, H.; Huang, Y. R.; Sun, W. Emodin ameliorates cisplatin-induced apoptosis of rat renal tubular cells in vitro by activating autophagy. *Acta Pharmacol. Sin.* **2016**, *37*, 235−245.
(28) Shrimali, D.; Shanmugam, M. K.; Kumar, A. P.; Zhang, J. W.; Tan, B. K. H.; Ahn, K. S.; Sethi, G. Targeted abrogation of diverse signal transduction cascades by emodin for the treatment of inflammatory disorders and cancer. *Cancer Lett.* **2013**, *341*, 139−149.
(29) Liu, X. Y.; Liu, Y. Q.; Qu, Y.; Cheng, M. C.; Xiao, H. B. Metabolomic profiling of emodin-induced cytotoxicity in human liver cells and mechanistic study. *Toxicol. Res.* **2015**, *4*, 948−955.
(30) Chen, Y. Y.; Chiang, S. Y.; Lin, J. G.; Yang, J. S.; Ma, Y. S.; Liao, C. L.; Lai, T. Y.; Tang, N. Y.; Chung, J. G. Emodin, Aloe-emodin and Rhein Induced DNA Damage and Inhibited DNA Repair Gene Expression in SCC-4 Human Tongue Cancer Cells. *Anticancer Res.* **2010**, *30*, 945−951.
(31) Chang, M. H.; Huang, F. J.; Chan, W. H. Emodin induces embryonic toxicity in mouse blastocysts through apoptosis. *Toxicology* **2012**, *299*, 25−32.
(32) Zawilska, J. B.; Wojcieszak, J.; Olejniczak, A. B. Prodrugs: a challenge for the drug development. *Pharmacol. Rep.* **2013**, *65*, 1−14.
(33) Li, N. N.; Lin, J.; Gao, D.; Zhang, L. M. A macromolecular prodrug strategy for combinatorial drug delivery. *J. Colloid Interface Sci.* **2014**, *417*, 301−309.
(34) Li, D.; Lu, B.; Huang, Z. J.; Xu, P. H.; Zheng, H.; Yin, Y. H.; Xu, H. X.; Liu, X.; Chen, L. Y.; Lou, Y. C.; Zhang, X. Q.; Xiong, F. L. A novel melphalan polymeric prodrug: Preparation and property study. *Carbohydr. Polym.* **2014**, *111*, 928−935.
(35) Bui, D. T.; Nicolas, J.; Maksimenko, A.; Desmaele, D.; Couvreur, P. Multifunctional squalene-based prodrug nanoparticles for targeted cancer therapy. *Chem. Commun.* **2014**, *50*, 5336−5338.
(36) Cao, B.; Xiao, F. F.; Xing, D.; Hu, X. L. Polyprodrug Antimicrobials: Remarkable Membrane Damage and Concurrent Drug Release to Combat Antibiotic Resistance of Methicillin-Resistant *Staphylococcus aureus*. *Small* **2018**, *14*, No. 1802008.
(37) Ji, H. W.; Dong, K.; Yan, Z. Q.; Ding, C.; Chen, Z. W.; Ren, J. S.; Qu, X. G. Bacterial Hyaluronidase Self-Triggered Prodrug Release for Chemo-Photothermal Synergistic Treatment of Bacterial Infection. *Small* **2016**, *12*, 6200−6206.
(38) Yao, Y.; Zhao, L. Y.; Yang, J. J.; Yang, J. Glucose-Responsive Vehicles Containing Phenylborate Ester for Controlled Insulin Release at Neutral pH. *Biomacromolecules* **2012**, *13*, 1837−1844.
(39) Cai, T. T.; Lei, Q.; Yang, B.; Jia, H. Z.; Cheng, H.; Liu, L. H.; Zeng, X.; Feng, J.; Zhuo, R. X.; Zhang, X. Z. Utilization of H-bond interaction of nucleobase Uralic with antitumor methotrexate to design drug carrier with ultrahigh loading efficiency and pH-responsive drug release. *Regener. Biomater.* **2014**, *1*, 27−35.
(40) Yang, B.; Lv, Y.; Zhu, J. Y.; Han, Y. T.; Jia, H. Z.; Chen, W. H.; Feng, J.; Zhang, X. Z.; Zhuo, R. X. A pH-responsive drug nanovehicle constructed by reversible attachment of cholesterol to PEGylated poly(L-lysine) via catechol-boronic acid ester formation. *Acta Biomater.* **2014**, *10*, 3686−3695.
(41) Zhou, P.; Wu, S.; Hegazy, M.; Li, H.; Xu, X. J.; Lu, H.; Huang, X. Engineered borate ester conjugated protein-polymer nanoconjugates for pH-responsive responsive drug delivery. *Mater. Sci. Eng., C* **2019**, *104*, No. 109914.
(42) Kim, S. H.; Sharker, S. M.; In, I.; Park, S. Y. Surface patterned pH-sensitive fluorescence using beta-cyclodextrin functionalized poly(ethylene glycol). *Carbohydr. Polym.* **2016**, *147*, 436−443.
(43) Wang, B.; Chen, L. M.; Sun, Y. J.; Zhu, Y. L.; Sun, Z. Y.; An, T. Z.; Li, Y. H.; Lin, Y.; Fan, D. P.; Wang, Q. Development of phenylboronic acid-functionalized nanoparticles for emodin delivery. *J. Mater. Chem. B* **2015**, *3*, 3840−3847.
(44) Jia, H. Z.; Zhang, W.; Wang, X. L.; Yang, B.; Chen, W. H.; Chen, S.; Chen, G.; Zhao, Y. F.; Zhuo, R. X.; Feng, J.; Zhang, X. Z. Polymeric assembly of hyperbranched building blocks to establish tunable nanoplatforms for lysosome acidity-responsive gene/drug co-delivery. *Biomater. Sci.* **2015**, *3*, 1066−1077.
(45) Zhang, P.; Xu, Q. N.; Li, X. F.; Wang, Y. X. pH-responsive polydopamine nanoparticles for photothermally promoted gene delivery. *Mater. Sci. Eng., C* **2020**, *108*, No. 110396.
(46) Matsumoto, A.; Sato, N.; Kataoka, K.; Miyahara, Y. Noninvasive Sialic Acid Detection at Cell Membrane by Using Phenylboronic Acid Modified Self-Assembled Monolayer Gold Electrode. *J. Am. Chem. Soc.* **2009**, *131*, 12022−12023.
(47) Yang, B.; Jia, H. Z.; Wang, X. L.; Chen, S.; Zhang, X. Z.; Zhuo, R. X.; Feng, J. Self-Assembled Vehicle Construction via Boronic Acid Coupling and Host-Guest Interaction for Serum-Tolerant DNA Transport and pH-Responsive Drug Delivery. *Adv. Healthcare Mater.* **2014**, *3*, 596−608.
(48) Hu, X.; Liu, R. L.; Zhang, D.; Zhang, J.; Li, Z. H.; Luan, Y. X. Rational Design of an Amphiphilic Chlorambucil Prodrug Realizing Self-Assembled Micelles for Efficient Anticancer Therapy. *ACS Biomater. Sci. Eng.* **2018**, *4*, 973−980.
(49) Liu, L.; Xing, Y.; Zhang, H.; Liu, R. L.; Liu, H. J.; Xia, N. Amplified voltammetric detection of glycoproteins using 4-mercaptophenylboronic acid/biotin-modified multifunctional gold nanoparticles as labels. *Int. J. Nanomed.* **2014**, *9*, 2619−2626.
(50) Cai, Q. Q.; Yang, S. L.; Zhang, C.; Li, Z. M.; Li, X. D.; Shen, Z. Q.; Zhu, W. P. Facile and Versatile Modification of Cotton Fibers for Persistent Antibacterial Activity and Enhanced Hygroscopicity. *ACS Appl. Mater. Interfaces* **2018**, *10*, 38506−38516.
(51) Cao, W. B.; Yue, L.; Khan, I. M.; Wang, Z. P. Polyethylenimine modified MoS_2 nanocomposite with high stability and enhanced photothermal antibacterial activity. *J. Photochem. Photobiol., A* **2020**, *401*, No. 112762.
(52) Xiao, F. F.; Cao, B.; Wen, L. W.; Su, Y. H.; Zhan, M. X.; Lu, L. G.; Hu, X. L. Photosensitizer conjugate-functionalized poly(hexamethylene guanidine) for potentiated broad-spectrum bacterial inhibition and enhanced biocompatibility. *Chin. Chem. Lett.* **2020**, *31*, 2516−2519.
(53) Shi, S.; Zhu, X. C.; Guo, Q. F.; Wang, Y. J.; Zuo, T.; Luo, F.; Qian, Z. Y. Self-assembled mPEG-PCL-g-PEI micelles for simultaneous codelivery of chemotherapeutic drugs and DNA: synthesis and characterization in vitro. *Int. J. Nanomed.* **2012**, *7*, 1749−1759.
(54) Veiseh, O.; Kievit, F. M.; Mok, H.; Ayesh, J.; Clark, C.; Fang, C.; Leung, M.; Arami, H.; Park, J. O.; Zhang, M. Q. Cell transcytosing poly-arginine coated magnetic nanovector for safe and effective siRNA delivery. *Biomaterials* **2011**, *32*, 5717−5725.
(55) Xu, Z. H.; Jin, J. F.; Siu, L. K. S.; Yao, H.; Sze, J.; Sun, H. Z.; Kung, H. F.; Poon, W. S.; Ng, S. S. M.; Lin, M. C. Folic acid conjugated mPEG-PEI600 as an efficient non-viral vector for targeted nucleic acid delivery. *Int. J. Pharm.* **2012**, *426*, 182−192.
(56) Peng, Q.; Chen, F. J.; Zhong, Z. L.; Zhuo, R. X. Enhanced gene transfection capability of polyethylenimine by incorporating boronic acid groups. *Chem. Commun.* **2010**, *46*, 5888−5890.
(57) Wu, L. L.; Zou, Y.; Deng, C.; Cheng, R.; Meng, F. H.; Zhong, Z. Y. Intracellular release of doxorubicin from core-crosslinked polypeptide micelles triggered by both pH and reduction conditions. *Biomaterials* **2013**, *34*, 5262−5272.
(58) Xun, W.; Wang, H. Y.; Li, Z. Y.; Cheng, S. X.; Zhang, X. Z.; Zhuo, R. X. Self-assembled micelles of novel graft amphiphilic copolymers for drug controlled release. *Colloids Surf., B* **2011**, *85*, 86−91.

https://doi.org/10.1021/acsomega.1c00606
ACS Omega 2021, 6, 8672−8679